CHAPTER – VI

CHAPTER - VI

6 SIMPLIFIED ANALYSIS METHOD FOR EXAFS SPECTRA USING MATHCAD PROGRAMMING

6.1 Introduction

X-ray absorption fine structure (XAFS) is a powerful and versatile technique for studying structures of materials in chemistry, physics, biology, and other fields. its widely-used technique for determining the local geometric and/or electronic structure of matter. XAFS spectra are sensitive to the formal oxidation state, coordination chemistry, and the distances, coordination number and species of the atoms immediately surrounding the selected element. XAFS provides a practical, and relatively simple, way to determine the chemical state and local atomic structure for a selected atomic species. XAFS can be used in a variety of systems and bulk physical environment. XAFS is routinely used in a wide range of scientific fields, including biology, environmental science, catalysts research, and material scienceX-ray absorption fine structure (XAFS) refers to modulation in X-ray absorption coefficient just above the X-ray absorption edge.

XAFS is often divided into two regions, XANES (which lies within the first 30 eV from the edge position) and EXAFS (which lies beyond 30 eV from the absorption edge).EXAFS is applicable to both condensed matter and gases.

The phenomenon of extended X-ray absorption fine structure (EXAFS), which refers to the oscillatory variation of the X-ray absorption as a function of photon energy beyond the absorption edge, has been discussed in chapter I of this thesis. EXAFS has become the technique of choice for local structural investigations in a diverse range of material systems. This technique has also proved very useful, while studying the chemical reactions of matter under extreme conditions of temperature and pressure.

The noticeable advantage of XAFS technique is that we may use the X-ray absorption spectroscopy a bulk probe to investigate surface effects. In particular, the technique permits the analysis of buried interfaces systems that are difficult to be analyzed even with more sophisticated surface investigation equipments. Applications of EXAFS can be found in literature on a variety of fields, namely, chemical reactions

at the solid state[161], surface treatments[162] and structural studies of thin films[163]. A variety of spectrometers dedicated to this method are available on the major synchrotron radiation sources[164] . The theory of X-ray absorption spectroscopy is presently well-understood[165] and it permits the quantitative determination of local structure parameters both from the near edge region as well as from the extended zone.

In the present chapter, a newly approached method has been employed for analysis of the EXAFS spectra and determination of first shell bond length. Extended X-ray absorption fine structure (EXAFS) data has been theoretically generated using standard EXAFS equation, employing computer software MathCAD, for the first coordination shell around the absorbing atom. For this calculation, the required phase shift has been taken from the experimental data given in chapter IV and chapter V of this thesis. The backscattering amplitude has been assumed to be equal to one.

The proposed method has been applied to the copper complexes and copper salts which have been given in table 6.1 and table 6.2 respectively.

The theoretical EXAFS data have been obtained using MathCAD programming. The theoretical EXAFS data has been Fourier transformed. The first shell bond lengths have been obtained from the Fourier transforms. These bond lengths have been compared with the bond lengths determined by using L.S.S.[166] , Levy's[167] and Lytle's methods[168] for copper salts and copper complexes.

6.2 Methodology

A simple and innovative method of analysis of EXAFS data for extracting first shell bond length around the absorbing atom has been developed by the author and is being described here. The method utilizes the use of the easily available MathCAD

---

[161] Heald S. M. and Stern E. A., 1977, Phys. Rev. B, **16**, 5549.
d'Acapito F., Ghigna P., Alessandri I., Cardelli A., and Davoli I., 2003, Nucl.Instrum. Methods Phys. Res. B, **200**, 421.

[162] Lutzenkirchen H. and Frahm R., 2005, Physica B Amsterdam, **357**, 213.
Hecht D., Frahm R., and Strehblow H. H., 1996, J. Phys. Chem., **100**, 10831.

[163] Jiang D. T., Alberding N., Seary A. J. and Crozier E. D., 1988, Rev. Sci. Instrum., **59**, 60.
Cartechini L., miliani C., brunetti G., sgamellotti A., altavilla C., ciliberto E. and D'acapito F., 2008, Appl. Phys. A, **92**, 243.

[164] Oyanagi H., Owen I., Grimshaw M., Head P., Martin M. and Saito M., 1995, Rev. Sci. Instrum., **66**, 5477.
Hecht D., Frahm R., and Strehblow H. H., 1996, J. Phys. Chem., **100**, 10831.
Jiang D. T., Alberding N., Seary A. J. and Crozier E. D., 1988, Rev. Sci. Instrum., **59**, 60.
Pizzini S., Roberts K. J., Greaves G. N., Harris N., Moore P., Pantos E., and Oldman R. J, 1989, Rev. Sci. Instrum., **60**, 2525.
Acapito D., Davoli I., Ghigna P., and Mobilio S., 2003, J. Synchrotron Radiat., **10**, 260.

[165] Flores L., Ansell S., Bowron D. T., Diaz-Moreno S., Ramos S., and Munoz-Paez A., 2007, Rev. Sci. Instrum., **78**, 013109.

[166] Lytle F. W., Sayers D. E. and Stern E. A., 1975(a), Phys. Rev. B, **11,** 4825

[167] Levy R. M., 1965, J. Chem. Phys., **43**, 1846.

[168] Lytle F.W., 1966, Advances in X-ray Analysis, **9**,398.

software. The theoretical spectrum is generated by using the EXAFS eqn. (1.10). The theoretically generated EXAFS spectrum is Fourier transformed. The position of the peak in the Fourier transform gives the value of the first shell bond length. The details of the calculations for generating the theoretical EXAFS spectrum are given in this section.

6.2.1 The EXAFS equation

The EXAFS equation (1.10) has been described in detail in section 1.8.3 of chapter I of this thesis. In this chapter, the equation has been used extensively. Hence, the equation is discussed in brief in this section.

The attenuation of X-rays by matter generally follows the relation $I = I_0 e^{-\mu x}$, where $\mu(E)$ is the X-ray absorption coefficient, I_0 is the incident intensity, I is the transmitted intensity and x is the sample thickness. The EXAFS is defined as the normalized oscillatory part of $\mu(E)$ and is given by eqn. (1.2):

$$\chi(E) = [\mu(E) - \mu_0(E)] / \Delta\mu_0$$

where $\mu_0(E)$ is the smoothly varying portion of $\mu(E)$ past the absorption edge and $\Delta\mu_0$ is the edge step. The $\chi(E)$ data is converted to $\chi(k)$ data by using the relation:

$$k = [0.263(E - E_0)]^{1/2}$$

(6.1)

where E_0 is the threshold energy. This relation is similar to the equations (1.5), (1.6) and (1.14).

The EXAFS equation that has become the standard for current work is the eqn. (1.10):

$$\chi(k) = \sum_j \frac{(N_j S_0^2) F_j(k)}{kR_j^2} \times \sin[2kR_j + \delta_j(k)] \times \exp(-2\sigma_j^2 k^2) \times \exp[-2R_j / \lambda(k)]$$

The subscript j denotes the various scattering paths. N_j is the number of atoms in the j^{th} coordination shell, R_j is the average radial distance to the j^{th} atom, σ_j^2 is mean square deviation about the bond length. S_0^2 is the passive electron reduction factor and accounts for the slight relaxation of the remaining electrons in the presence of the core-hole vacated by the photoelectron. S_0^2 usually has a value between 0.7 and 1.0 and is different for different elements. The function $F_j(k)$ is the photoelectron

backscattering amplitude and $\delta_j(k)$ is the scattering phase shift for each scattering path. $\lambda(k)$ is the photoelectron mean free path which is dominated by lifetime of the excited state.

For generating the theoretical EXAFS spectrum, the EXAFS equation described above is written in MathCAD program. The various inputs required in this equation are: N_j, S_0^2, $F_j(k)$, R_j, δ_j, σ_j and $\lambda(k)$.

6.2.2 Values of input parameters

The values of N_j, σ_j and $\lambda(k)$ have been taken from crystallographic data for copper metal (Stern et al., 1975). The values of S_0^2 and $F_j(k)$ have been taken as one. δ_j has been written as $2(\alpha_j + \beta_j)$. The values of R_j, α_j and β_j for Copper complexes and Cu(II) Salts have been reported in table 6.3 and table 6.4 respectively. These values have been taken as inputs to the EXAFS equation. The values of α_j and β_j are determined using equation (1.19) of chapter I, i.e., by the graphical method outlined by Lytle, Sayers and Stern (L.S.S. method)[169]. For obtaining the $\chi(k)$ EXAFS data at different values of k, the value of wave vector k has been varied at equal interval of 0.05 Å.

6.2.3 Fourier transform of the theoretical EXAFS spectrum and determination of first shell bond length

One of the earliest analyses of EXAFS was based on the Fourier transform (FT) of the data expressed in momentum space. The absolute value of the transform was found to peak at distances shifted from the known values by 0.2 - 0.5Å. By correcting for these shifts using systems with known distances, bond length information can be extracted[170]. The Fourier transformation of $k^n \chi(k)$ in momentum (k) space over the finite k range k_{min} to k_{max} gives rise to a modified radial distribution function $\phi_n(R')$ in distance (R') space.

$$\phi_n(R') = \frac{1}{\sqrt{2\pi}} \int_{k_{min}}^{k_{max}} w(k) k^n \chi(k) e^{2ikR'} dk \qquad (6.2)$$

[169] Lytle F. W., Sayers D. E. and Stern E. A., 1975(a), Phys. Rev. B, **11,** 4825.
[170] Stern E.A., 1974, Phys. Rev. B, **10** 3027.
Sayers D.E., Stern E.A., and Lytle F.W., 1971, Phys. Rev. Lett., **27**, 1204.
Lee P.A. and Beni G., 1977, Phys. Rev. B, **15**, 2862.

To locate the position of each peak in $\phi_n(R')$, it is necessary to understand the phase shift more fully. The linear k dependent term shifts the frequency of the sine wave of EXAFS equation from R_i to $(R_i - \alpha_i)$. In the Fourier transform, this has the effect of shifting all the peaks towards the origin by α, where α amounts to 0.2 ~ 0.5 Å depending upon, among others, the elements involved, the E_0 chosen, and the weighting scheme. α can be obtained from model compounds and transferred to the unknown systems to predict distances.

From χ(k), the radial distribution function $|\phi_w(R)|$ can be derived using eqn. (6.2). The maxima of this function are generated by shells of scattering atoms surrounding the absorbing atom. The positions of the peaks in $|\phi_w(R)|$ are shifted compared to true distances due to contribution of the scattering phases that depend on k. When the theoretically generated EXAFS data is Fourier transformed, the Fourier transform peak for the first shell occur at $R_1' = R_1 - \alpha_1$, where R_1' is the measured distance and R_1 is the true distance. For generating the Fourier transform of the theoretical EXAFS spectrum, the eqn. (6.2) described above is written in MathCAD program.

A Fourier transform of χ (k) will have peaks at $R_j' = R_j - \alpha_j$ corresponding to average radial distance (R) of the j^{th} atom from the absorbing atom. Thus, the positions of the peaks in the Fourier transform of the EXAFS signal are related to the distance between the absorbing atom and the neighbouring atoms, and the height is related to the number of neighbouring atoms at this distance. The distance found in the Fourier transform is about 0.2 - 0.5Å, shorter than the actual distance by α_j because of the phase shift. If this factor was absent, the peak in Fourier transform would have been a direct measure of R_j. Hence, to extract the information about the first shell bond length, the value of α_1 is added to the value of distance of the peak in the Fourier transform, i.e., R_1.

In the present chapter, this simplified method for theoretical analysis of EXAFS data has been applied to some copper (II) complexes and copper salts. The X-ray absorption measurements have been taken at the recently developed BL-8 dispersive EXAFS beam line at 2.5 GeV Indus-2 Synchrotron Source at RRCAT, Indore,The copper (II) complexes and copper(II) salts and their abbreviations are shown in table 6.1 and table 6.2 respectively..

6.3 Results and discussion

The calculated EXAFS features of the copper (II) complexes have been shown in figs 6.1(a-j) and that of copper (II) salts have been shown in figs 6.3(a-e) respectively. Figs 6.2 (a-j) and 6.4(a-e) give the magnitude of Fourier transform of the theoretical $\chi(k)$ versus k curves of figs 6.1 (a-j) and 6.3 (a-e) respectively.

The method employed in the present work for theoretical analysis of EXAFS data and determination of the structural parameters using MathCAD programming is simpler than commonly used IFEFFIT technique[171].

The bond lengths obtained from the present method of analysis of EXAFS data using MathCAD program for copper (II) complexes are tabulated in table 6.3. In this table are also given the values of bond lengths obtained using L.S.S., Lytle's and Levy's methods. It can be seen from this table that the values obtained by this simplified analysis method are comparable to those obtained by other methods.

Similarly, the bond lengths obtained for copper (II) salts from the analysis using MathCAD programming have been compared with the bond lengths obtained from L.S.S.[172], Lytle's[173] and Levy's[174] methods. The present results as well as those obtained obtained by the above three methods have been tabulated in table 6.4 for copper (II) salts. A perusal of tables 6.3 and 6.4 shows that the values obtained by this simplified analysis method are comparable to those obtained by other methods.

The method of analysis presented in this chapter has been successfully applied to the studied copper complexes. The method is simple and comparable to the rigorous theoretical methods. The present method of analysis also provides a physical picture of the X-ray absorption process. The present work brings out the effective use of the graphical method for extracting the phase parameters. The present method can be used for studying systems such as amorphous materials, metallic glasses, bio molecules etc. in which knowledge about the environment of atoms is desired.

6.4 Conclusions

The method described in this chapter for the analysis of EXAFS data is simple and straight forward, thereby providing a physical picture of the X-ray absorption process.

---

[171] Newville M., 2001, J. Synchrotron Rad., **8**, 322.
[172] Lytle F. W., Sayers D. E. and Stern E. A., 1975(a), Phys. Rev. B, **11,** 4825
[173] Lytle F.W., 1966, Advances in X-ray Analysis, **9**,398.
[174] Levy R. M., 1965, J. Chem. Phys., **43**, 1846.

The calculated EXAFS curves for copper (II) complexes and copper (II) salts have been found to be in good agreement with experimental EXAFS curves for all complexes and salts studied within experimental error. This means that the parameterized theoretical calculations of the EXAFS spectra described are in good agreement with physical reality. A perusal of the bond length values obtained from the analysis of EXAFS data by the present method using MathCAD programming indicates that the calculated values are in good agreement with the values obtained from L.S.S.[175], Levy's[176] and Lytle's[177] methods. The results show that the atomic distance of central atom with the first nearest neighbor has not been found to be affected significantly when the various substituents in the ligand are changed. The reason is that the substituents are not directly linked to the central atom.

[175] Lytle F. W., Sayers D. E. and Stern E. A., 1975(a), Phys. Rev. B, **11,** 4825
[176] Levy R. M., 1965, J. Chem. Phys., **43**, 1846.
[177] Lytle F.W., 1966, Advances in X-ray Analysis, **9**,398.

Table 6.1 Copper (II) complexes, abbreviation and molecular formula.			
S.No	**Complex name**	**Abbreviation**	**Molecular formula**
1.	Bis-pentanyl R(4-Nitro)- phenyldiazine Cu(II) bis-benzenediamine	Bisp(4-Nitro) pdCu(II)bisbd	$C_{32}H_{26}N_{10}O_4Cl_2Cu$
2.	Bis-pentanyl R(pure anilene)- phenyldiazine Cu(II) bis-benzenediamine	Bisp(pure anilene) pdCu(II)bisbd	$C_{32}H_{28}N_8Cl_2Cu$
3.	Bis-pentanyl R(2-anisidine)- phenyldiazine Cu(II) bis-benzenediamine	Bisp(2-anisidine) pdCu(II)bisbd	$C_{34}H_{32}N_8O_2Cl_2Cu$
4.	Bis-pentanyl R(4-chloro)- phenyldiazine Cu(II) bis-benzenediamine	Bisp(4-chloro) pdCu(II)bisbd	$C_{32}H_{26}N_8Cl_4Cu$
5.	Bis-pentanyl R(4-Bromo)- phenyldiazine Cu(II) bis-benzenediamine	Bisp(4-Bromo) pdCu(II)bisbd	$C_{32}H_{26}N_8Cl_2Br_2Cu$
6.	Bis-pentanyl R(2-chloro)- phenyldiazine Cu(II) bis-benzenediamine	Bisp(2-chloro) pdCu(II)bisbd	$C_{32}H_{26}N_8Cl_4Cu$
7.	Bis-pentanyl R(3-Nitro)- phenyldiazine Cu(II) bis-benzenediamine	Bisp(3Nitro)pdCu(II)bisbd	$C_{32}H_{26}N_{10}O_4Cl_2Cu$
8.	Bis-pentanyl R(2-Nitro)- phenyldiazine Cu(II) bis-benzenediamine	Bisp(2- Nitro) pdCu(II)bisbd	$C_{32}H_{26}N_{10}O_4Cl_2Cu$
9.	Bis-pentanyl R(4-anisidine)- phenyldiazine Cu(II) bis-benzenediamine	Bisp(4-anisidine) pdCu(II)bisbd	$C_{32}H_{26}N_8Cl_4Cu$
10.	Bis-pentanyl R(Aceto-p-Toludine)- phenyldiazine Cu(II) bis-benzenediamine	Bisp(Aceto-p-Toludine)pdCu(II)bisbd	$C_{36}H_{32}N_8O_2Cl_2Cu$

Table 6.2 Copper (II) salts, abbreviation and molecular formula.		
S. No.	**Salt**	**Molecular Formulae**
1.	**Copper Chloride**	**$CuCl_2.2H_2O$**
2.	**Copper Sulphate**	**$CuSO_4.5H_2O$**
3.	**Copper Bromide**	**$CuBr_2$**
4.	**Copper Acetate**	**$Cu(CH_3COO)_2.H_2O$**
5.	**Copper Nitrate**	**$Cu(NO_3)_2.3H_{2O}$**

Table 6.3 First shell metal-ligand bond length in (Å) for copper (II) complexes					
Complex/parameter	**R_{Levy}**	**α**	**β**	**R_{FT}(using mathcad)**	**R_{FT}(using Athena)**
Bisp(4-Nitro)pdCu(II)bisbd	**1.50**	**.38**	**-2.27**	**1.08**	**1.10**
Bisp(pureanilene)pdCu(II)bisbd	**1.82**	**.26**	**-3.12**	**1.56**	**1.46**
Bisp(2-anisidine)pdCu(II)bisbd	**1.50**	**.41**	**-2.11**	**1.04**	**1.11**
Bisp(4-chloro) pdCu(II)bisbd	**1.52**	**.40**	**-2.15**	**1.08**	**1.11**
Bisp(4-Bromo) pdCu(II)bisbd	**1.38**	**.06**	**-2.04**	**1.32**	**1.61**
Bisp(2-chloro) pdCu(II)bisbd	**1.51**	**.20**	**-2.29**	**1.32**	**1.30**
Bisp(3-Nitro)pdCu(II)bisbd	**1.61**	**.27**	**-2.29**	**1.33**	**1.32**
Bisp(2-Nitro) pdCu(II)bisbd	**1.52**	**.18**	**-2.40**	**1.33**	**1.29**
Bisp(4-anisidine)pdCu(II)bisbd	**1.50**	**.40**	**-2.13**	**1.04**	**1.16**
Bisp(AcetoToludine)pdCu(II)bisbd	**1.50**	**.40**	**-2.18**	**1.04**	**1.16**

Table 6.4 First shell metal-ligand bond length in (Å) for copper (II) salts					
Complex/parameter	**R_{Levy}**	**α**	**B**	**R_{FT}(using mathcad)**	**R_{FT}(using Athena)**
Copper Chloride	**1.53**	**.19**	**-2.51**	**1.37**	**1.37**
Copper Sulphate	**1.48**	**.15**	**-2.38**	**1.33**	**1.39**
Copper Bromide	**1.54**	**.14**	**-2.55**	**1.38**	**2.22**
Copper Acetate	**1.48**	**.18**	**-2.40**	**1.30**	**1.22**
Copper Nitrate	**1.93**	**.65**	**-2.43**	**1.28**	**1.41**

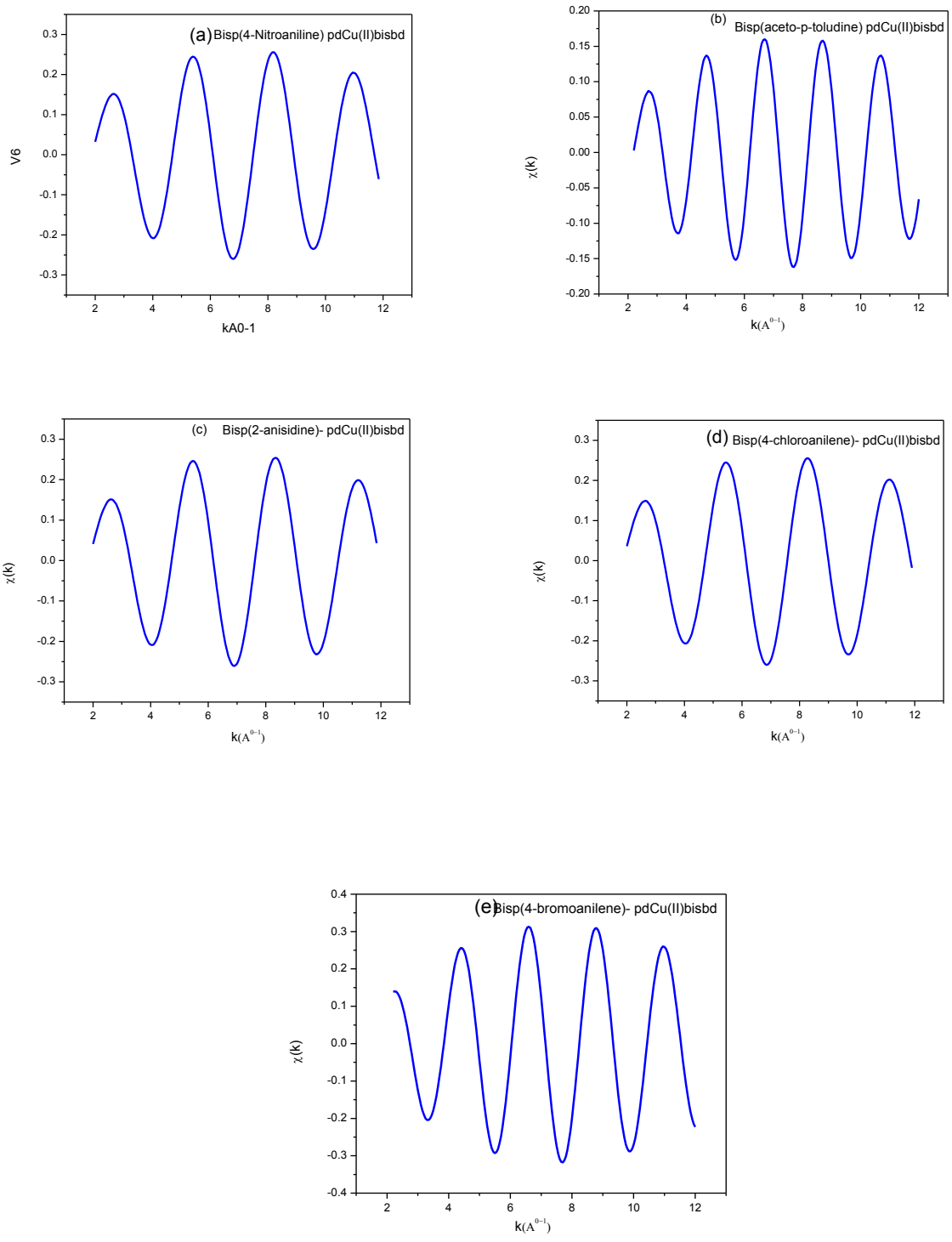

Figure 6-1 Theoretically calculated χ (k) versus k curves for the copper (II) complexes.

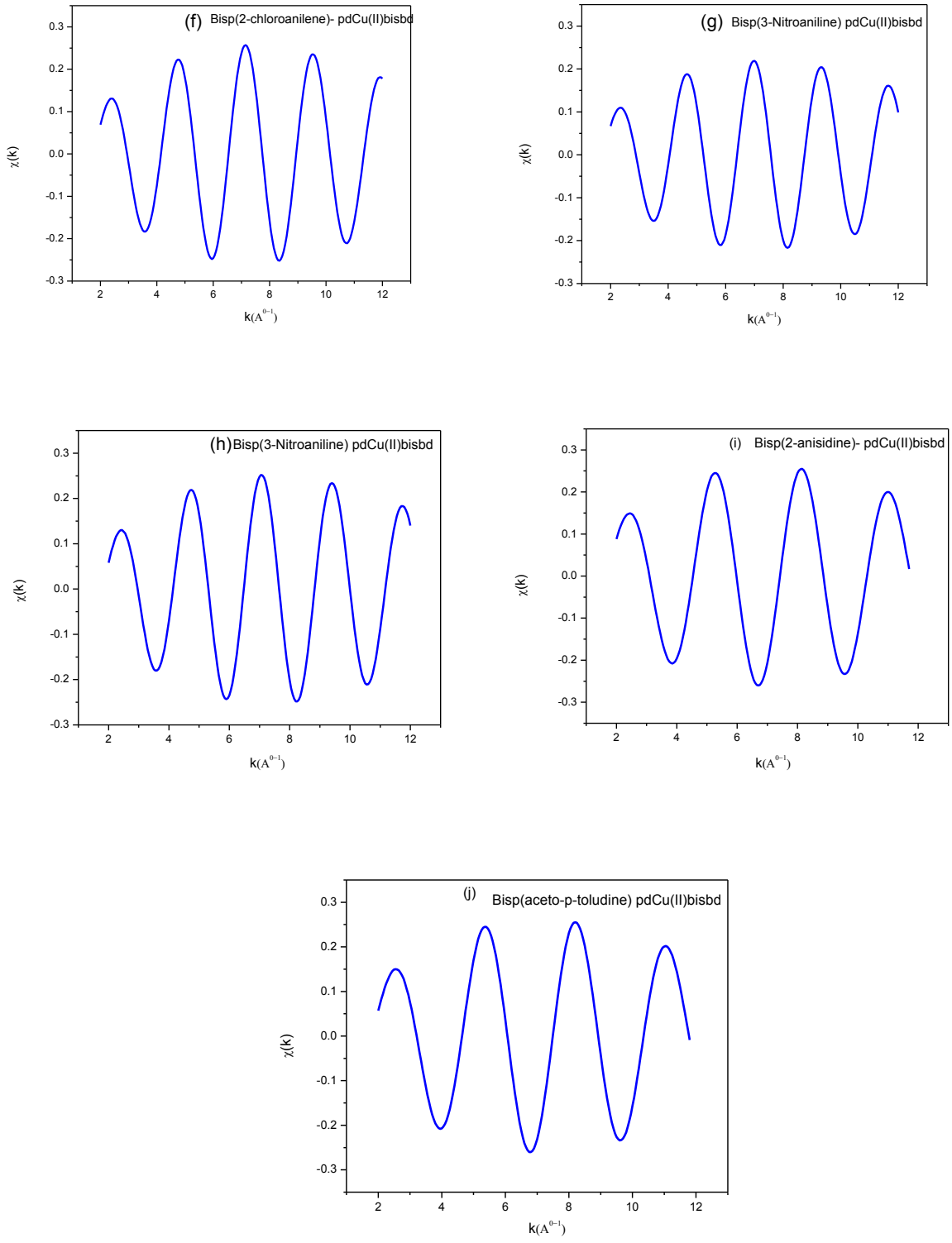

Fig. 6-1 Theoretically calculated χ (k) versus k curves for the copper (II) complexes.

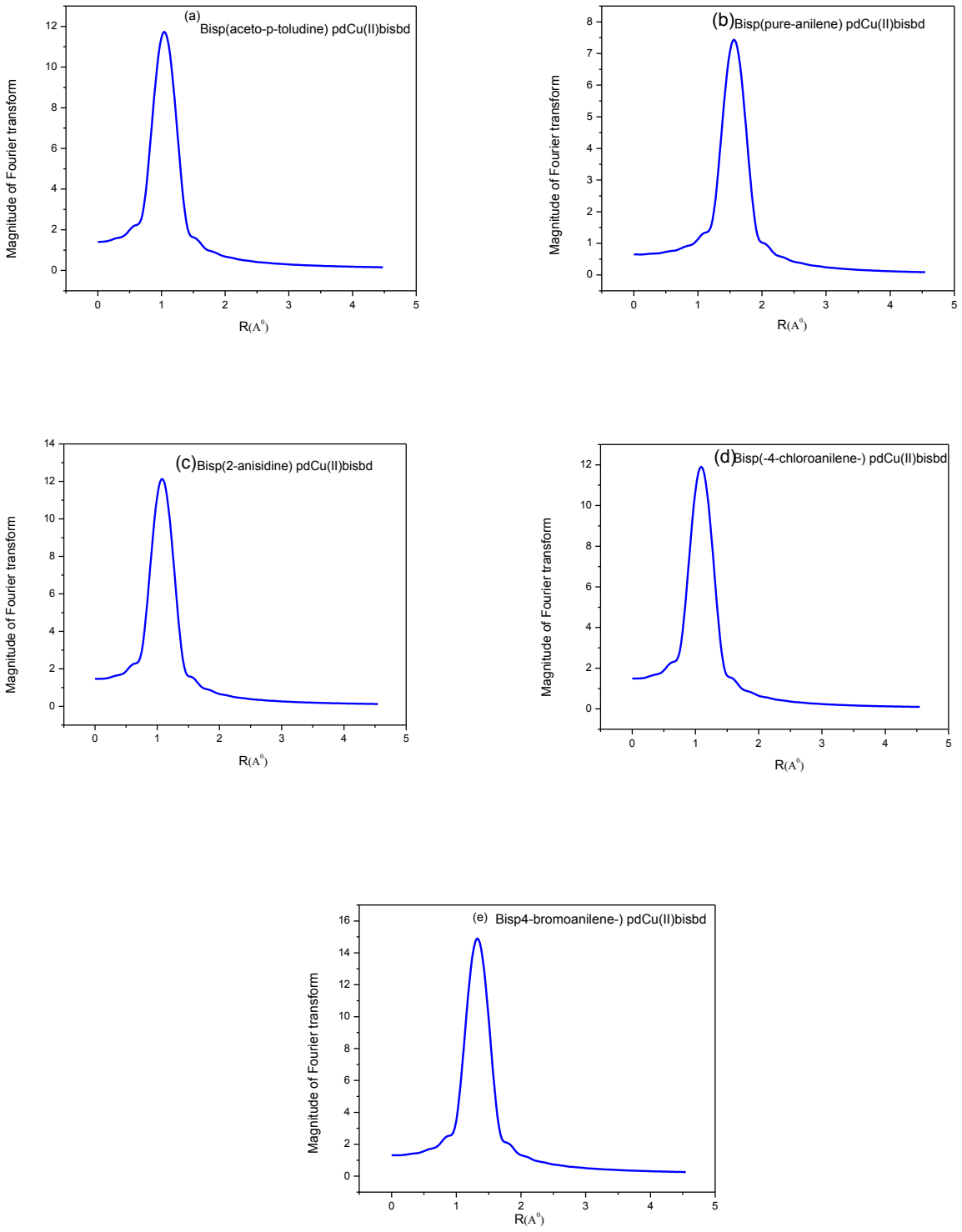

Figure 6-2 Magnitude of Fourier transform of the χ(k) versus k curves of fig. 6.1.

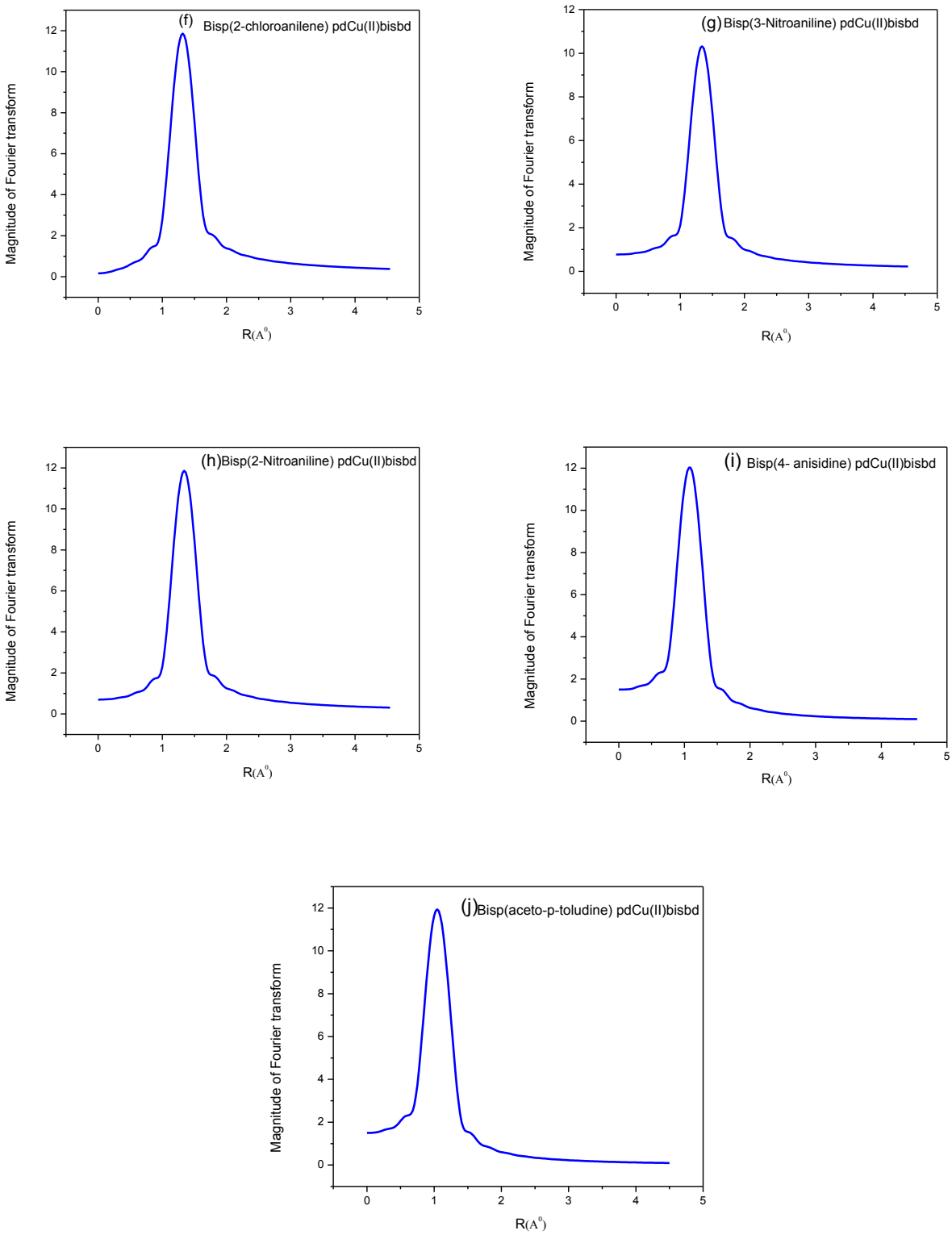

Fig. 6-2 Magnitude of Fourier transform of the χ(k) versus k curves of fig. 6.1.

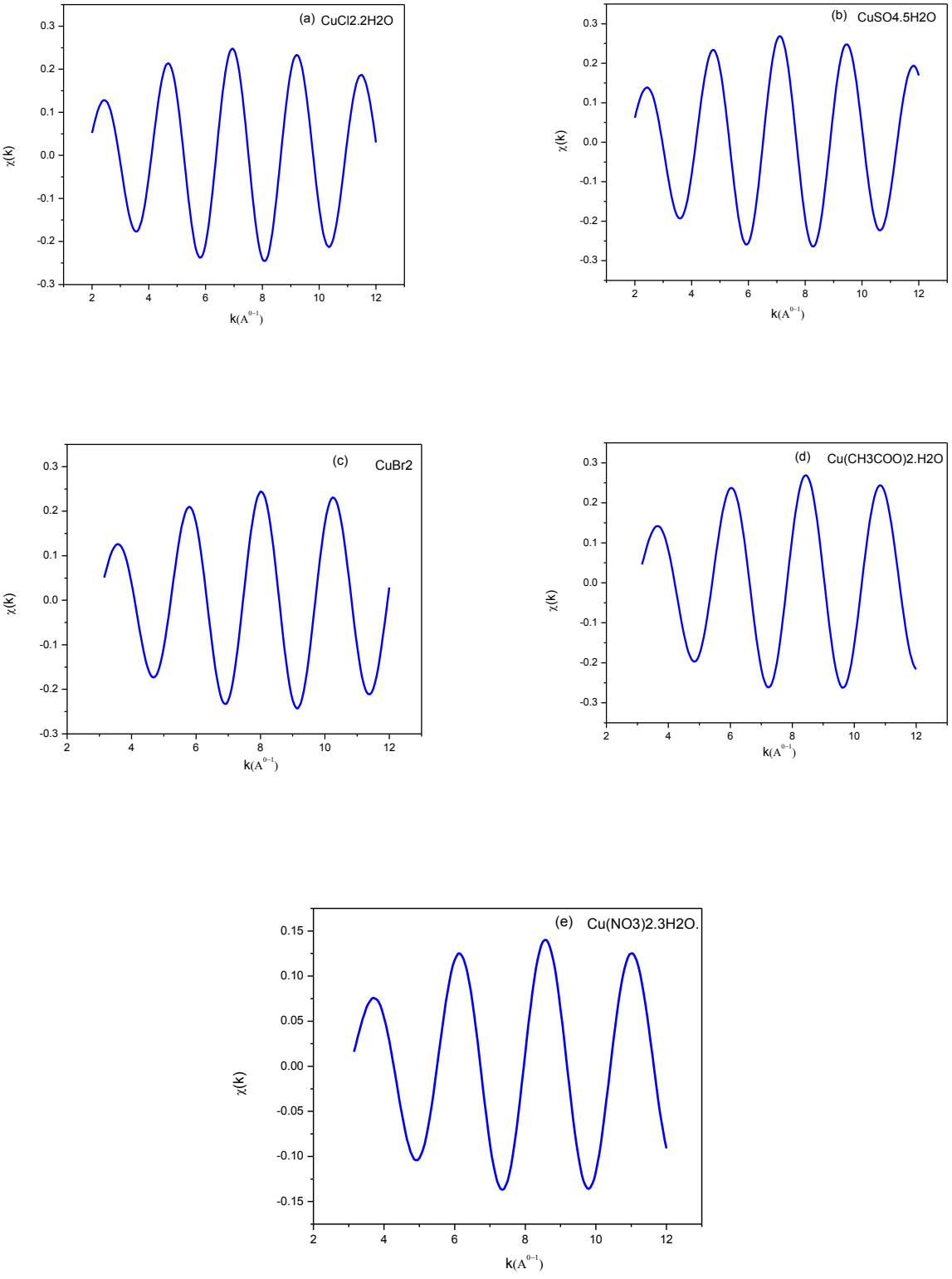

Figure 6-3 Theoretically calculated χ(k) versus k curves for the copper (II) Salts.

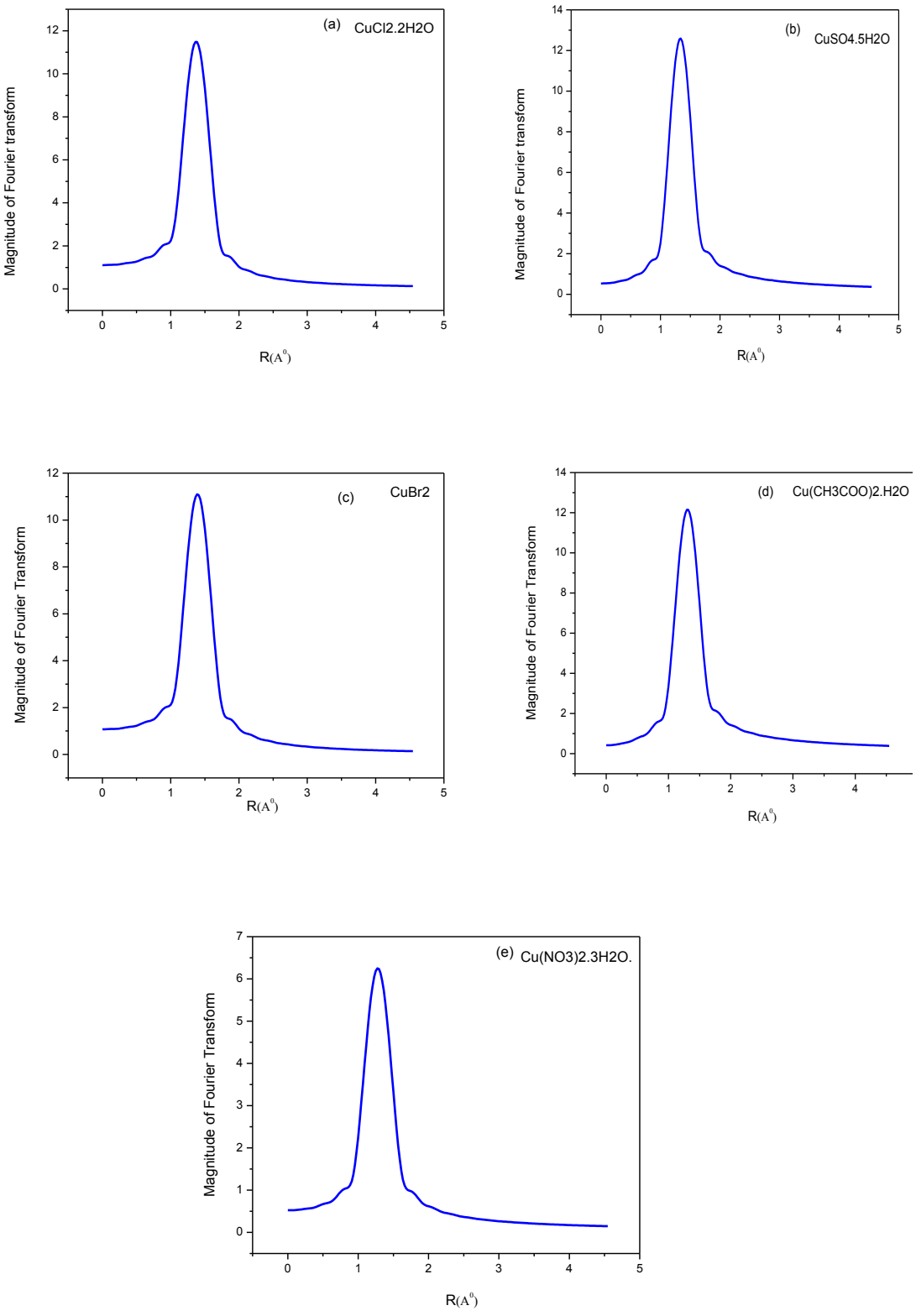

Figure 6-4 Magnitude of Fourier transforms of the χ (k) versus k curves of fig. 6.3.